
The dynamics of the DNA denaturation transition

TITUS S. VAN ERP¹ AND MICHEL PEYRARD²

¹ *Centrum voor Oppervlaktechemie en Katalyse, KU Leuven, Kasteelpark Arenberg 23, B-3001 Leuven, Belgium*

² *Laboratoire de Physique, Ecole Normale Supérieure de Lyon, 46 allée d'Italie, 69364 Lyon Cedex 07, France*

PACS 87.15.H- – Dynamics of biomolecules

PACS 82.20.Pm – Rate constants, reaction cross sections, and activation energies

PACS 87.14.gk – DNA

Abstract – The dynamics of the DNA denaturation is studied using the Peyrard-Bishop-Dauxois model. The denaturation rate of double stranded polymers decreases exponentially as function of length below the denaturation temperature. Above T_c , the rate shows a minimum, but then increases as function of length. We also examine the influence of sequence and solvent friction. Molecules having the same number of weak and strong base-pairs can have significantly different opening rates depending on the order of base-pairs.

For decades, experimental and theoretical scientists have been fascinated by the thermal DNA denaturation [1]. It is biologically relevant since the opening of the double helix is an important step for the transcription of the genetic code [2] but it is also becoming important for nanotechnology as DNA is now used for its self-assembly properties [3], to create nanodevices [4] or to design molecular memories [5]. The different AT and GC base-pairs (bps) are intra-connected by two and three hydrogen-bonds, respectively. Denaturation experiments, in which UV absorbance is measured as function of temperature, show discrete steps associated to the sequential opening of soft and stiff regions in the DNA sequence. These regions mainly differ by their density of weak AT-versus strong GC-bps, but also the specific order is important [6]. On the other hand, large homogeneous chains denature in a single step within a very small temperature interval, a remarkable realization of an effectively one-dimensional phase transition [7].

Theoretically, the statistics of DNA have been modeled via Ising type models [8] in which each bp is given a value 0 or 1 depending on whether it is open or closed. This approach allows the study of extremely large sequences but cannot be used to study dynamics. This has been the principle motivation for Peyrard, Bishop and Dauxois to develop a continuous model (PBD) [9]. The PBD model is computationally somewhat more expensive than the Ising type models, but still quite efficient due to its mesoscopic character. As a result, the PBD model is very well suited to study dynamics of reasonably long DNA

molecules at timescales that are not reachable with full-atom simulations [10]. The PBD model, therefore, meets our requirements that we need to study the dynamics of the DNA denaturation transition. In specific, we want to understand how the rate of full denaturation depends on several parameters such as length, sequence, solvent friction, and temperature.

The PBD model has revealed a rich spectrum of dynamical phenomena such as the existence of nonlinear localized modes [11]. Ironically, most studies on the PBD model that apply specific types of dynamics, such as Nose-Hoover, Brownian motion, and Langevin (sometimes even using a configurational dependent friction parameter [12]), have reported on equilibrium properties like the fraction of open bp's at a given temperature. These properties, in principle, do not depend on the dynamics [13]. So far, the study on actual dynamics has been limited to the local opening of DNA [15] or denaturation at elevated temperatures [14]. For applications such as nanodevices [4] on molecular memories [5], the timing becomes important.

The dynamics of full denaturation is difficult to access using standard MD as it is a rare event on the timescale that is achievable by molecular simulations. Transition interface sampling (TIS) [16] and the more recent Replica Exchange TIS [17] are powerful techniques to beat this timescale problem. However, a very efficient implementation of the reactive flux (RF) method [18] can treat the PBD model even more efficiently [17]. The RF method starts from the Transition State Theory (TST) expression, but corrects for correlated recrossings via a dynamical

factor, the transmission coefficient. Unlike TST, the RF method provides an exact expression for the rate constant that is independent to the choice of reaction coordinate (RC). In Ref. [17], we showed how the free energy and the transmission coefficient can be calculated very efficiently by exploiting specific peculiarities of the PBD model. Using this approach, we can achieve rates far below 10^{-15} ns⁻¹ or, in other words, relaxation times of several days or even years. We are not aware of any mesoscopic modeling approach that is able to reach such timescales. In this letter, we apply this method to determine the dependence of the denaturation rate of double stranded DNA as function of its length, the temperature and solvent friction, the content of weak AT versus strong CG bp's, and their specific order.

The PBD describes the DNA molecule as an one-dimensional chain of effective atom compounds yielding the relative base-pair separations y_i from the ground state positions. The total potential energy U for an N base-pair DNA chain is given by $U(\{y_i\}) = V_1(y_1) + \sum_{i=2}^N V_i(y_i) + W(y_i, y_{i-1})$ with

$$V_i(y_i) = D_i \left(e^{-a_i y_i} - 1 \right)^2 \quad (1)$$

$$W(y_i, y_{i-1}) = \frac{1}{2} K \left(1 + \rho e^{-\alpha(y_i + y_{i-1})} \right) (y_i - y_{i-1})^2$$

The first term V_i is the Morse potential describing the hydrogen bond interaction between bases on opposite strands. D_i and a_i determine the depth and width of this potential for the AT and GC base-pairs. Note that the PBD model does not distinguish between A- and T-nor between G- and C-bases. The second term W is the stacking interaction. The ρ -term makes that the effective strength of the stacking interaction drops from $K(1 + \rho)$ down to K whenever either y_i or y_{i-1} becomes significantly larger than $1/\alpha$. This effect mimics the decrease of overlap between π - electrons when one of two neighboring bases move out of stack and it is thanks to this that the sharp phase transition in long homogeneous chains can be reproduced.

Our results are primary focused on the parameter set of Campa and Giansanti [19] with $K = 0.025$ eV/Å², $\rho = 2$, $\alpha = 0.35$ Å⁻¹, $D_{AT} = 0.05$ eV, $D_{GC} = 0.075$ eV, $a_{AT} = 4.2$ Å⁻¹, $a_{GC} = 6.9$ Å⁻¹. However, we will also shortly investigate the more recent parameter set by Theodorakopoulos [20]: $K = 0.00045$ eV/Å², $\rho = 50$, $\alpha = 0.2$ Å⁻¹, $D_{AT} = 0.1255$ eV, $D_{GC} = 0.1655$ eV, $a_{AT} = 4.2$ Å⁻¹, $a_{GC} = 6.9$ Å⁻¹. Particular of this data-set is the very high ρ value which should reflect the large difference in persistence length of single stranded and double stranded DNA [21]. $\lambda \equiv \min\{y_i\}$ was chosen as reaction coordinate RC [17] and $y_0 = 1$ Å as the opening threshold. Henceforth, $y_i > y_0$ implies that base-pair i is open and $\lambda > y_0$ that the complete molecule is denatured.

The RF method expresses the overall reaction rate as an equilibrium probability density to be at a surface on the barrier (here defined by $\lambda(\{y_i\}) = y_0$), under the condition

that the system is at the reactant side of this surface, times a dynamical transmission factor.

$$k = P(\lambda = y_0 | \lambda \leq y_0) \times R \quad \text{with} \quad R = \left\langle \dot{\lambda} \theta(\dot{\lambda}) h_{0,y_0}^b \right\rangle_{\lambda=y_0} \quad (2)$$

The dynamical factor R is called is the unnormalized transmission coefficient. The brackets with subscript denote an ensemble average that is constrained on the surface $\lambda(\{y_i\}) = y_0$. It is calculated by releasing dynamical trajectories forward and backward in time starting from a proper equilibrium ensemble of configuration points on this surface and Maxwell-Boltzmann distributed velocities. h_{0,y_0}^b is a binary function that is 1 if the backward trajectory from such a point evolves to the minimum of the Morse potential ($\lambda = 0$ Å) without recrossing the initial surface ($\lambda = y_0$). Otherwise it is 0. Since this surface is at the frontier of what is considered to be the product state, no forward trajectory is needed as in Ref. [23], since $\lambda(\{y_i\}) = y_0$ and $\dot{\lambda} > 0$ implies that the product state will be entered within an infinitesimal small time step. This procedure is sketched in fig. 1.

Assuming $h_{0,y_0}^b = 1$ whenever $\dot{\lambda} > 0$ would result into the TST approximation of the reaction rate. In practice, $h_{0,y_0}^b = 0$ for the vast majority of trajectories though its average value remains measurable for this RC due to the flat plateau of the Morse potential. The time duration of these trajectories are much shorter than the actual relaxation time that relates to the long time evolution of the system having relatively small oscillations. Therefore, even though the very large fluctuations of these short trajectories are at the limit of what the PBD can describe accurately, their short duration, with respect to the actual relaxation time, make quantitative rate calculations reliable. Also the fact that we stop our trajectories whenever $y_i > y_0$ for all i is reasonable. Besides that the PBD model isn't too accurate beyond this point, it is expected that the chance of reclosing is even smaller in a more accurate three-dimensional model. We can, therefore, assume that the system is committed to the denatured state beyond this point and it is therefore sufficient to stop the trajectory whenever the y_0 transition surface is crossed. Still, it is fair to say that our approach and RC will probably not work for more elaborated potentials that contain explicit potential barriers for reclosing [24] since it will result in $R \ll 1$.

The equilibrium density is related to the free energy via $F(\lambda) = -k_B T \ln P(\lambda)$ with k_B the Boltzmann constant and T the temperature in Kelvin. The surface does not necessarily have to be at the local maximum of the free energy profile, the transition state (TS), though this is generally the most efficient choice since it maximizes the transmission R . In our case the surface $\lambda(\{y_i\}) = y_0$ is slightly beyond the TS at the beginning of the denaturation state or product state region. This has, however, no effect on the final results since the transmission coefficient and probability density are like communicating

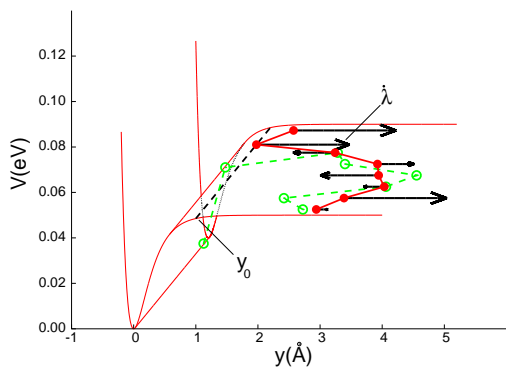


Fig. 1: (color online) The above figure illustrates an example configuration (solid red spheres) at the surface $\lambda(\{y_i\}) = y_0$ that was generated by our algorithm for a homogeneous $N = 8$ AT-chain. It has one particle that is exactly at y_0 while $y_i > y_0$ for all others. The arrows envision the corresponding Maxwellian velocities. Each of these sampled phases points will give a single value x that is either zero or positive. If $\dot{\lambda}$ (which is simply the velocity of the particle that is exactly on the surface) equals less than zero, then $x = 0$. If $\dot{\lambda} > 0$, all velocities of the system will be reversed and the dynamics are propagated using the Langevin dynamics. These dynamics are continued until one particle reaches the well ($y_i < 0$ for one particle or $\dot{\lambda} < 0$) or until all particles move beyond the initial surface ($y_i > y_0$ for all particles or $\dot{\lambda} > y_0$). In the last case x is assigned zero again. In the first case x equals the initial velocity $\dot{\lambda}$. The final configuration is shown by the green open circles. A particle at the end of the chain has moved inside the well of the Morse potential (hence $x = \dot{\lambda}$ for this case). This event implies a commitment to the natured state; this particle will quickly pull the others inside the well and a rapid recrossing with the y_0 surface is highly unlikely after this point. The unnormalized transmission coefficient is the average of the sampled values x : $R = \bar{x}$.

vessels; a too high value for P (or too low value of ΔF) is compensated by a lower transmission R . Therefore, the calculated rate values are insensitive to the exact location of the transmission surface.

Because of the first neighbor character of the PBD model, the free energy or probability density $P(\lambda = y_0 | \lambda \leq y_0)$ can be computed very efficiently by means of an iterative numerical integration scheme [17].

$$P = \frac{\sum_i \int dy_1 \dots dy_N \delta(y_i - y_0) \prod_{j \neq i} \theta(y_j - y_0) e^{-\beta U(\{y_i\})}}{\int dy_1 \dots dy_N (1 - \prod_k \theta(y_k - y_0)) e^{-\beta U(\{y_i\})}} \quad (3)$$

Now, as the integrals of Eq. (3) are all of a special factorial form [22], we can apply the direct integration method of Ref. [22] using an integration step of $dy = 0.05 \text{ \AA}$ and integration boundaries $|y_i - y_{i-1}| < d = \sqrt{2} |\ln \tau| / \beta K$ and $-1/a_{AT} \ln \left[\sqrt{|\ln \tau| / \beta D_{AT}} + 1 \right] < y_i < y_0 + \sqrt{N}d$. The tolerance τ is set to 10^{-40} which implies that all contributions of $e^{-\beta V(\{y_i\})}$ lower than this value are neglected. The very low value of K in the parameter set of [20]

with respect to [19] implies significant larger integration boundaries and a 50 times higher computational cost.

In the next step, we need to generate a representative set of configurations on the surface $\lambda(\{y_i\}) = y_0$. Also this can be achieved very effectively for this particular model and RC. We make use of the fact that ensemble constraint to this surface is identical to a freely moving chain on a translational invariant potential U' with $U'(\{y_i\}) \equiv U(\{y_i - \lambda(\{y_i\}) + y_0\})$ [22]. Therefore, we generate the required surface points by running a MD simulation using potential U' , save every 1000th time step to dissolve correlations. Then, we shift these configurations back to the surface $\lambda(\{y_i\}) = y_0$. From each point, we release a backward trajectory using normal potential U and determine $\dot{\lambda}\theta(\dot{\lambda})h_{0,y_0}^b$. We averaged over 10^6 trajectories using a time step of 1 fs and bp masses of 300 amu. The temperature was controlled using Langevin dynamics with a friction coefficient of $\gamma = 50 \text{ ps}^{-1}$ unless stated otherwise.

It is important to stress that factor P is purely a thermodynamic property (i. e. independent of γ or masses) while R depends on the full dynamics. This methodology allows us for the first time to examine the theoretical PBD denaturation rates of long DNA molecules as function of sequence, solvent friction, temperature, and model parameters.

Fig. 2 shows the calculated denaturation rates of homo-

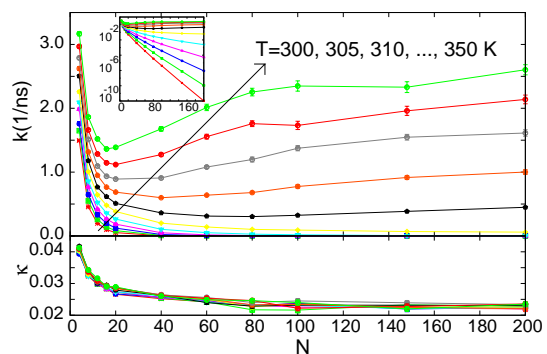


Fig. 2: (color online) Top: Denaturation rate of homogeneous AT chains as function of the number of bps N at different temperatures. Inset shows the same results in log-scale. Bottom: The corresponding transmission coefficients.

geneous A/T-DNA sequences of different lengths and temperatures. Below the critical denaturation temperature ($T_c \approx 325K$) the denaturation rate of the DNA molecule is exponentially decreasing as function of its length. Above T_c , there is an initial decrease as function of the number of bps N , but then starts to increase again. Both the depth and the position of the minimum decrease as function of temperature. This feature is mainly an effect of equilibrium statistical physics (factor P) rather than dynamics (factor R) as we can conclude from the lower panel of fig. 2. This panel shows the normalized transmission coefficient $\kappa \equiv R / \langle \dot{\lambda}\theta(\dot{\lambda}) \rangle = \sqrt{2\pi\beta m}R$ which is equivalent to

the true rate constant divided by the transition state theory (TST) value. The results show that, although κ is far smaller than one, it is more or less constant with respect of temperature and chain length. Only for short polymers $N < 20$ there is a noticeable upturn of κ . Henceforth, despite that TST overestimates the rate by more than a factor 40, the relative TST rates are approximately correct.

An increase of denaturation rate as function of its length is remarkable even for $T > T_c$. For macroscopic systems having two phases A and B , crossing the phase transition temperature coincides with a discontinuous jump of the equilibrium constant from zero to infinity. Since the equilibrium constant is related to the ratio of forward and backward rate constants, $k_{A \rightarrow B}/k_{B \rightarrow A}$ goes from zero to infinity in the limit $N \rightarrow \infty$ when T crosses T_c . Still, this does not imply that the absolute values of any of the two rates should increase as function of N . In fact, the decreasing denaturation time $\tau \sim 1/k$ as function of N is in contrast to the power-law scaling $\tau \propto N^{2.57}$ of a non-equilibrium case study [14].

To examine the effect of temperature on the equilibrium statistics, fig. 3 shows the free energy $F(\lambda') =$

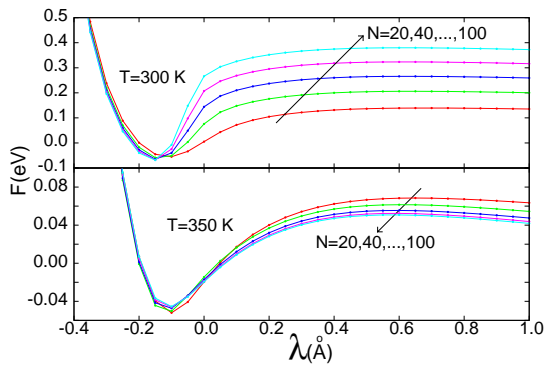


Fig. 3: (color online) The free energy profile as function of the RC for homogeneous A/T chains of different lengths and temperatures $T = 300$ K (top) and $T = 350$ K (bottom).

$-\ln [P(\lambda = \lambda' | \lambda < y_0) / P^0] / \beta$ with $P^0 = 1/\text{\AA}$ being an arbitrary reference density. At temperature $T = 300$ K the free energy barrier is clearly increasing as function of chain length while it is slightly decreasing at $T = 350$ K. The longer polymers profit from the larger entropy gain at high T .

In fig. 4, we examined the effect of heterogeneities in the DNA sequences at room temperature conditions ($T = 300$ K). The red and blue curve represent the denaturation rate for the homogeneous A/T and G/C-sequences. The green curve in the middle corresponds to sequences where the first half is purely A/T and the other half G/C. All curves become straight lines for sufficiently large N which implies an exponential dependence on the chain length. Linear fits in the log-plot reveal that $k \approx ab^N$ with $a(1/\text{ns}), b = 0.240, 0.897$ for the A/T- and $0.436, 0.678$ for the G/C-chain. The mixed AG-sequence has

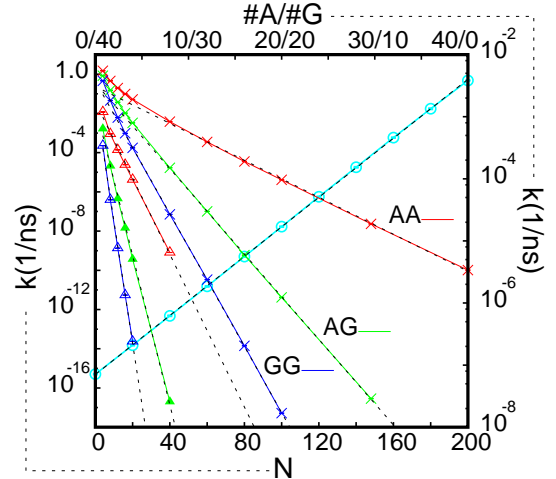


Fig. 4: (color online) Denaturation rate versus the number bps for homogeneous A/T- (red line) and G/C-chains (blue) and a sequence having $N/2$ consecutive A's followed by $N/2$ consecutive G's (green). Crosses correspond to the parameter set of Ref. [19], triangles correspond to Ref. [20]. Blue line indicates the rate (right and top axis) for a mixed 40 bp chain having M consecutive A- followed by $40-M$ G-bps. Dashed black lines are best linear fits in the log-plot.

$a = 0.346$ and $b = 0.778$. The latter value is very close to $\sqrt{b(A) \times b(G)} = 0.780$ which suggest $k \propto b(A)^{N_A} b(G)^{N_G}$ as a general rule for a mixed sequence where N_A and N_G are the number of A/T- or G/C-bps. The results based on the alternative parameter set of Ref. [20] show the same trend but predicts denaturation rates that are orders of magnitude lower. The linear fits give $a, b = 0.039, 0.639$ for A/T, $0.048, 0.240$ for GC-, and $0.0249, 0.415$ for the mixed chain. The latter is again very close to $\sqrt{b(A) \times b(G)}$ which corroborates with the above. In fig. 4 we also show the denaturation rate for a polymer of fixed $N = 40$ length as function of the A,G-content using parameter set [19]. Like before, the order of the polymer is such that the A- and G-bps are placed consecutively at opposite sides. Making the linear fit in the log-plot shows that $k \approx 7.06(1/\text{ns})1.31^{N_A}$ which is again in excellent agreement with the above rule since $b(A)/b(G) = 1.32$.

In Fig. 5 we examined the influence of the friction constant γ . As the dynamics do not change the equilibrium distribution they can only have an effect on κ . In agreement with previous finding, we see that the transmission coefficient is hardly affected by the polymer length, the type of bps and temperature. In conclusion, κ is mainly determined by the friction coefficient γ . At high friction we notice a standard Kramer's behavior [25] $\kappa \propto 1/\gamma$ which is somewhat surprising given the exotic nature of the RC that depends on all y_i coordinates in a discontinuous way. Contrary to Kramer's theory, κ converges to values in the range $0.38 - 0.48$ and does not approach 1 in the limit $\gamma \rightarrow 0$.

Finally, we also examined the influence of the order of the sequence on the denaturation rate. In fig. 6 we show

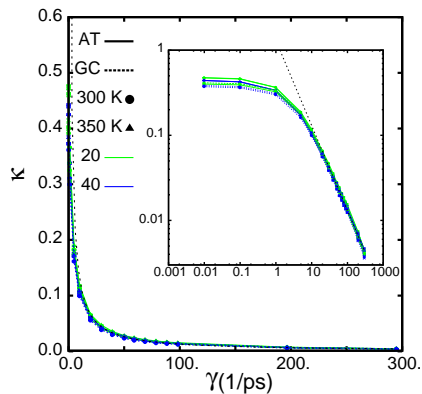


Fig. 5: (color online) Transmission coefficient versus the friction coefficient γ for a homogeneous A- (solid line) or G- (dashed line) at temperatures $T = 300$ K (spheres) or 350 K (triangles) consisting of 20 (green) or 40 (blue) bps. Inset shows the same results in a log-log plot. Dashed black line corresponds to the fit $\kappa(\gamma) = 1.3 \text{ ps}^{-1}/\gamma$.

normalized denaturation rates as function of N for sequences that all contain 50% A- and 50% G-bases. The computed rate constant where normalized by the values of fig. 4. Hence, all values are relative to a chain having all A's and all G's at one side of the polymer. We call this the AAGG-sequence after the $N = 4$ polymer having this characteristics. Besides the AAGG-sequence, we ex-

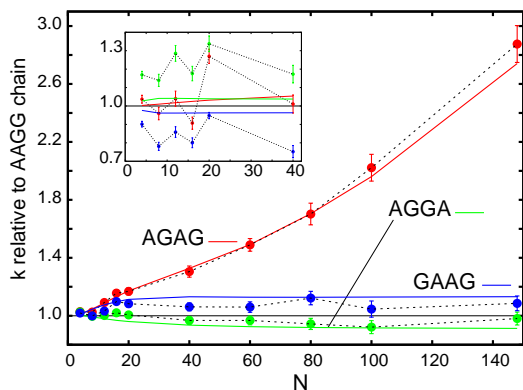


Fig. 6: (color online) Relative denaturation rates versus chain length for DNA sequences having 50% A- and 50% G-bps. The curves only differ in the ordering of bps. All values are normalized by the chain having all A's at one side and the G's at the other side ("AAGG" after the $N=4$ bp chain). The alternating sequence AGAG (red) is shown together with the sequences having an A- (blue) or G-block (green) in the middle, respectively GAAG and AGGA. Full circles with error-bars show the results of the full calculation while the solid line is the result when transmission coefficients κ would be considered to be identical for all sequences. Inset shows the same results for the alternative parameter set of Ref. [20].

amined the alternating sequence AGAG, the "weak-block in the middle" sequence GAAG, and the "strong-block in the middle" sequence AGGA. The results were computed

in two ways i) using the full rates, ii) using the probabilities densities P alone. The second approach basically assumes that all transmission coefficients are identical for all sequences which seems to be right considering previous conclusions and has the advantage that its result is not affected by statistical uncertainties.

Fig. 6 shows that the AGAG sequence gives significant faster denaturation compared to the AAGG-chain and this effect increases with chain length. The GAAG-chain is second best being approximately 13% faster than AAGG for $N > 20$ without further increase as function of chain length. Conversely, the AGGA-sequence is about 10% slower than AAGG. Naturally, the bases at the end of the polymer are the most easy to open. Apparently, the best way to profit from this effect is to put the bases at the end that are difficult to open otherwise, but an even distribution of the G-bases is by far the best.

The results of the alternative parameter set, however, (inset in fig. 6) seems to give a somewhat different conclusion. The statistical error-bars are much larger for this parameter set due to the very weak coupling K which increases the accessible phase-space. Still, AGGA and GAAG seem to be reversed regardless method and i) or ii) is applied. The AGGA seem to denature even faster than the AGAG-chain though this might be just a statistical fluctuation. If we consider the method ii), we see that the red curve starts to grow as function of N and surpasses the AGGA result at $N = 40$. Therefore, we believe that the alternating sequence has the fastest denaturation irrespective of the parameter set for sufficiently large N . Besides their interest for studies involving real devices, those results on the effect of the sequence are important because they provide experimentally testable data [26] that discriminate between two parameter sets that give very similar equilibrium properties. This offers a unique possibility to validate model parameters.

In conclusion, we have utilized an innovative approach to study the denaturation rate as function of different parameters. This has resulted in several predictions which can be tested experimentally. DNA models, giving similar results regarding statistics, can differ fundamentally when denaturation are concerned. Therefore, our methodology in combination with experiments provides an additional dimension to probe the validity of DNA models and to improve them. This will be a significant step forward in understanding the sequence-dependent dynamics of DNA which play a crucial role in several biological processes and new DNA-based devices for which the time response is important.

TSvE acknowledges the Methusalem funding (CASAS) by the Flemish government.

REFERENCES

- [1] THOMAS R., *Gene*, **135** (1993) 77.
- [2] BENHAM C. J., *Proc. Natl. Acad. Sci. USA*, **90** (1993) 2999.
- [3] GOODMAN R. P., SCHAAP A. T., TARDIN C. F., ERBEN C. M., BERRY R. M., SCHMIDT C. F. and TURBERFIELD A. J., *Science*, **310** (2005) 1661-1665
- [4] KOMIYA K., YAMAMURA M. and ROSE J. A., *Nucleic Acids Res.*, **38** (2010) 4539.
- [5] TAKINOUE M. and SUYAMA A., *Chem-Bio Informatics J.*, **4** (2004) 93; TAKINOUE M. and SUYAMA A., *Small*, **2** (2006) 1244.
- [6] DORNBERGER U., LEIJON M. and FRITZSCHE H., *J. Biol. Chem.*, **274** (1999) 6957.
- [7] INMAN R. B. and BALDWIN R. L., *J. Mol. Biol.*, **8** (1964) 452; PEYRARD M. and DAUXOIS T., *Math. Comp. Sim.*, **40** (1996) 305.
- [8] POLAND D. and SCHERAGA H. A., *J. Chem. Phys.*, **45** (1996) 1456.
- [9] DAUXOIS T., PEYRARD M. and BISHOP A. R., *Phys. Rev. E*, **47** (1993) R44.
- [10] VÁRNASI P. and ZAKRZEWSKA K., *Nucleic Acids Res.*, **32** (2004) 4269.
- [11] DAUXOIS T., PEYRARD M. and WILLIS C. R., *Physica D*, **57** (1992) 267; CUEVAS J., ARCHILLA J. F. R., GAIDIDEI Y. B. and ROMERO F. R., *Physica D*, **163** (2002) 106.
- [12] DAS T. and CHAKRABORTY S., *EPL*, **83** (2008) 48003.
- [13] VAN ERP T. S., CUESTA-LOPEZ S., HAGMANN J.-G. and PEYRARD M., *EPL*, **85** (2009) 68003.
- [14] BAIESI M., BARKEMA G. T., CARLON E. and PANJA D., *J. Chem. Phys.*, **133** (2010) 154907.
- [15] ALEXANDROV B. S., GELEV V., YOO S. W., BISHOP A. R., RASMUSSEN K. O., KIM O. and USHEVA A., *PLoS Comput. Biol.*, **5** (2009) e1000313.
- [16] VAN ERP T. S., MORONI D. and BOLHUIS P. G., *J. Chem. Phys.*, **118** (2003) 7762.
- [17] VAN ERP T. S., *Phys. Rev. Lett.*, **98** (2007) 268301.
- [18] FRENKEL D. and SMIT B., *Understanding molecular simulation*, 2nd ed. (Academic Press, San Diego, CA) 2002.
- [19] CAMPA A. and GIANSAANTI A., *Phys. Rev. E*, **58** (1998) 3585.
- [20] THEODORAKOPOULOS N., *Phys. Rev. E*, **82** (2010) 021905.
- [21] BAUMANN C., SMITH S., BLOOMFIELD V. and BUSTAMANTE C., *Proc. Natl. Acad. Sci. USA*, **94** (1997) 6185.
- [22] VAN ERP T. S., CUESTA-LOPÈZ S., HAGMANN J.-G. and PEYRARD M., *Phys. Rev. Lett.*, **95** (2005) 218104.
- [23] VAN ERP T. S., *J. Chem. Phys.*, **125** (2006) 174106.
- [24] PEYRARD M., CUESTA-LOPEZ S. and JAMES G., *Nonlinearity*, **21** (2008) T91.
- [25] HANGGI P., TALKNER P. and BORKOVEC M., *Rev. Mod. Phys.*, **62** (1990) 251.
- [26] BONNET G., KRICHEVSKY O. and LIBCHABER A., *Proc. Natl. Acad. Sci. USA*, **95** (1998) 8602; ALTAN-BONNET G., LIBCHABER A. and KRICHEVSKY O., *Phys. Rev. Lett.*, **90** (2003) 138101.